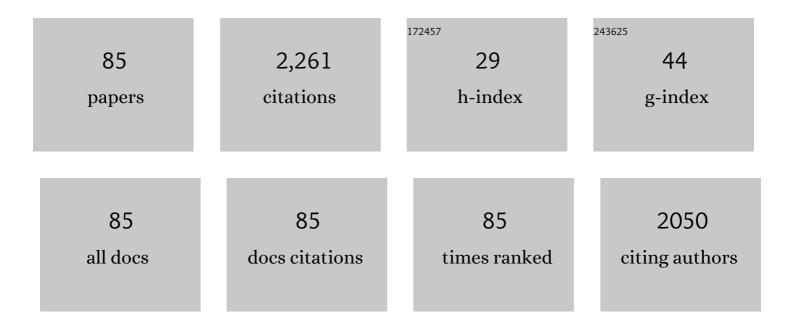
Huaiyu He

List of Publications by Year in descending order

Source: https://exaly.com/author-pdf/4735456/publications.pdf Version: 2024-02-01



Ηιιλινιι Ηε

#	Article	IF	CITATIONS
1	Binary mixing of lithospheric mantle and asthenosphere beneath Tengchong volcano, SE Tibet: evidence from noble gas isotopic signatures. International Geology Review, 2023, 65, 236-252.	2.1	2
2	New geochronology of the Lower Cretaceous in the Luanping Basin, northern Hebei: Age constraints on the development of early Jehol Biota. Palaeogeography, Palaeoclimatology, Palaeoecology, 2022, 586, 110768.	2.3	7
3	In situ detection of water on the Moon by the Chang'E-5 lander. Science Advances, 2022, 8, eabl9174.	10.3	28
4	Helium, neon and argon in alkaline basalt-related corundum megacrysts: Implications for their origin and forming process. Geochimica Et Cosmochimica Acta, 2022, , .	3.9	2
5	The exceptionally preserved Early Cretaceous "Moqi Fauna―from eastern Inner Mongolia, China, and its age relationship with the Jehol Biota. Palaeogeography, Palaeoclimatology, Palaeoecology, 2022, 589, 110824.	2.3	8
6	High-precision geochronology of the Early Cretaceous Yingcheng Formation and its stratigraphic implications for Songliao Basin, China. Geoscience Frontiers, 2022, 13, 101386.	8.4	11
7	Magnetostratigraphy of the Upper Cretaceous Nenjiang Formation in the Songliao Basin, northeast China: Implications for age constraints on terminating the Cretaceous Normal Superchron. Cretaceous Research, 2022, 135, 105213.	1.4	4
8	Magmatic chlorine isotope fractionation recorded in apatite from Chang'e-5 basalts. Earth and Planetary Science Letters, 2022, 591, 117636.	4.4	14
9	Rapid drift of the Tethyan Himalaya terrane before two-stage India-Asia collision. National Science Review, 2021, 8, nwaa173.	9.5	46
10	Interpreting and reporting 40Ar/39Ar geochronologic data. Bulletin of the Geological Society of America, 2021, 133, 461-487.	3.3	102
11	Neogene–quaternary magnetostratigraphy of the biogenic reef sequence of core NK–1 in Nansha Qundao, South China Sea. Science Bulletin, 2021, 66, 200-203.	9.0	16
12	SIMS U-Pb geochronology for the Jurassic Yanliao Biota from Bawanggou section, Qinglong (northern Hebei Province, China). International Geology Review, 2021, 63, 265-275.	2.1	6
13	Age determination of oriented rutile inclusions in sapphire and of moonstone from the Mogok metamorphic belt, Myanmar. American Mineralogist, 2021, 106, 1852-1859.	1.9	4
14	A Petrologic and Noble Gas Isotopic Study of New Basaltic Eucrite Grove Mountains 13001 from Antarctica. Minerals (Basel, Switzerland), 2021, 11, 279.	2.0	0
15	Plioâ€Pleistocene Establishment of Irtysh River in Junggar, Northwest China: Implications for Siberianâ€Arctic River System Evolution and Resulting Climate Impact. Geophysical Research Letters, 2021, 48, e2021GL093217.	4.0	5
16	Exploration of apatite (U Th)/He geochronological analysis of volcanic units in fossil-bearing strata of the Homa Peninsula, southwestern Kenya. Palaeogeography, Palaeoclimatology, Palaeoecology, 2021, 579, 110599.	2.3	1
17	New geochronological constraints for the Lower Cretaceous Jiufotang Formation in Jianchang Basin, NE China, and their implications for the late Jehol Biota. Palaeogeography, Palaeoclimatology, Palaeoecology, 2021, 583, 110657.	2.3	15
18	A dry lunar mantle reservoir for young mare basalts of Chang'e-5. Nature, 2021, 600, 49-53.	27.8	91

Ηυλιγύ Ηε

#	Article	IF	CITATIONS
19	Mesozoic Tectono-Thermal Event of the Qinshui Basin, Central North China Craton: Insights From Illite Crystallinity and Vitrinite Reflectance. Frontiers in Earth Science, 2021, 9, .	1.8	3
20	Magnetostratigraphy of the Upper Cretaceous and Lower Paleocene terrestrial sequence, Jiaolai Basin, eastern China. Palaeogeography, Palaeoclimatology, Palaeoecology, 2020, 538, 109451.	2.3	5
21	Reviewing Martian Atmospheric Noble Gas Measurements: From Martian Meteorites to Mars Missions. Geosciences (Switzerland), 2020, 10, 439.	2.2	6
22	The noble gases in five ordinary chondrites from Grove Mountains in Antarctica. Planetary and Space Science, 2020, 192, 105045.	1.7	6
23	The Potential of Marine Ferromanganese Nodules From Eastern Pacific as Recorders of Earth's Magnetic Field Changes During the Past 4.7ÂMyr: A Geochronological Study by Magnetic Scanning and Authigenic ¹⁰ Be/ ⁹ Be Dating. Journal of Geophysical Research: Solid Earth, 2020, 125, e2019IB018639.	3.4	12
24	The appearance and duration of the Jehol Biota: Constraint from SIMS U-Pb zircon dating for the Huajiying Formation in northern China. Proceedings of the National Academy of Sciences of the United States of America, 2020, 117, 14299-14305.	7.1	38
25	Early Cretaceous Terrestrial Milankovitch Cycles in the Luanping Basin, North China and Time Constraints on Early Stage Jehol Biota Evolution. Frontiers in Earth Science, 2020, 8, .	1.8	10
26	Implantation of Earth's Atmospheric Ions Into the Nearside and Farside Lunar Soil: Implications to Geodynamo Evolution. Geophysical Research Letters, 2020, 47, e2019GL086208.	4.0	11
27	New SIMS U-Pb geochronology for the Shahezi Formation from CCSD-SK-Ile borehole in the Songliao Basin, NE China. Science Bulletin, 2020, 65, 1049-1051.	9.0	17
28	Overview of lunar exploration and International Lunar Research Station. Chinese Science Bulletin, 2020, 65, 2577-2586.	0.7	23
29	Nature and evolution of the lithospheric mantle revealed by water contents and He-Ar isotopes of peridotite xenoliths from Changbaishan and Longgang basalts in Northeast China. Science Bulletin, 2019, 64, 1325-1335.	9.0	11
30	Response of the PRISMA-YBJ Detectors to Earthquakes. Bulletin of the Russian Academy of Sciences: Physics, 2019, 83, 607-610.	0.6	3
31	New geochronological constraints for the Upper Cretaceous Nenjiang Formation in the Songliao Basin, NE China. Cretaceous Research, 2019, 102, 160-169.	1.4	20
32	Oxygen isotopes in HED meteorites and their constraints on parent asteroids. Planetary and Space Science, 2019, 168, 83-94.	1.7	11
33	40Ar/39Ar dating results from the Shijiatun Formation, Jiaolai Basin: New age constraints on the Cretaceous terrestrial volcanic-sedimentary sequence of China. Cretaceous Research, 2018, 86, 251-260.	1.4	10
34	Noble gases in pyrites from the Guocheng-Liaoshang gold belt in the Jiaodong province: Evidence for a mantle source of gold. Chemical Geology, 2018, 480, 105-115.	3.3	37
35	⁴⁰ Ar/ ³⁹ Ar age of the onset of high-Ti phase of the Emeishan volcanism strengthens the link with the end-Guadalupian mass extinction. International Geology Review, 2018, 60, 1906-1917.	2.1	33
36	Timing of Secondary Hydrothermal Alteration of the Luobusa Chromitites Constrained by Ar/Ar Dating of Chrome Chlorites. Minerals (Basel, Switzerland), 2018, 8, 230.	2.0	0

Ηυλιγύ Ηε

#	Article	IF	CITATIONS
37	New SIMS U-Pb age constraints on the largest lake transgression event in the Songliao Basin, NE China. PLoS ONE, 2018, 13, e0199507.	2.5	13
38	He, Ar, and S isotopic compositions and origin of giant porphyry Mo deposits in the Lesser Xing'an Range–Zhangguangcai Range metallogenic belt, northeast China. Journal of Asian Earth Sciences, 2018, 165, 228-240.	2.3	11
39	Origin of ore-forming fluids of the Haigou gold deposit in the eastern Central Asian Orogenic belt, NE China: Constraints from H-O-He-Ar isotopes. Journal of Asian Earth Sciences, 2017, 144, 384-397.	2.3	31
40	A Potential (Uâ€Th)/He Zircon Reference Material from Penglai Zircon Megacrysts. Geostandards and Geoanalytical Research, 2017, 41, 359-365.	3.1	16
41	Recycled noble gases preserved in podiform chromitites from Luobusa, Tibet. Chemical Geology, 2017, 469, 97-109.	3.3	5
42	Petrographic shock indicators and noble gas signatures in a H and an L chondrite from Antarctica. Planetary and Space Science, 2017, 146, 20-29.	1.7	7
43	The Sources of Oreâ€forming Fluids from the Jinchang Gold Deposit, Heilongjiang Province, NE China: Constraints from the He–Ar Isotopic Evidence. Resource Geology, 2017, 67, 330-340.	0.8	13
44	Highâ€precision Uâ€Pb geochronology of the <scp>J</scp> urassic <scp>Y</scp> anliao <scp>B</scp> iota from <scp>J</scp> ianchang (western <scp>L</scp> iaoning <scp>P</scp> rovince, <scp>C</scp> hina): Age constraints on the rise of feathered dinosaurs and eutherian mammals. Geochemistry, Geophysics, Geosystems, 2016, 17, 3983-3992.	2.5	24
45	High-precision U–Pb geochronologic constraints on the Late Cretaceous terrestrial cyclostratigraphy and geomagnetic polarity from the Songliao Basin, Northeast China. Earth and Planetary Science Letters, 2016, 446, 37-44.	4.4	67
46	Volcanism in the Baikal rift: 40years of active-versus-passive model discussion. Earth-Science Reviews, 2015, 148, 18-43.	9.1	47
47	New evidence for the presence of Changbaishan Millennium eruption ash in the Longgang volcanic field, Northeast China. Gondwana Research, 2015, 28, 52-60.	6.0	33
48	A mixture of mantle and crustal derived He–Ar–C–S ore-forming fluids at the Baogutu reduced porphyry Cu deposit, western Junggar. Journal of Asian Earth Sciences, 2015, 98, 188-197.	2.3	14
49	Multiple isotope composition (S, Pb, H, O, He, and Ar) and genetic implications for gold deposits in the Jiapigou gold belt, Northeast China. Mineralium Deposita, 2014, 49, 145-164.	4.1	49
50	Geomagnetic field excursion recorded 17 ka at Tianchi Volcano, China: New ⁴⁰ Ar/ ³⁹ Ar age and significance. Geophysical Research Letters, 2014, 41, 2794-2802.	4.0	31
51	He and Ar isotope geochemistry of pyroxene megacrysts and mantle xenoliths in Cenozoic basalt from the Changle–Linqu area in western Shandong. Science Bulletin, 2014, 59, 396-411.	1.7	18
52	Superimposed tectono-metamorphic episodes of Jurassic and Eocene age in the jadeite uplift, Myanmar, as revealed by 40Ar/39Ar dating. Gondwana Research, 2014, 26, 464-474.	6.0	30
53	Age and origin of charoitite, Malyy Murun massif, Siberia, Russia. International Geology Review, 2014, 56, 1007-1019.	2.1	18
54	Tectonic and sedimentary evolution of the late Miocene–Pleistocene Dali Basin in the southeast margin of the Tibetan Plateau: Evidences from anisotropy of magnetic susceptibility and rock magnetic data. Tectonophysics, 2014, 629, 362-377.	2.2	20

Ηυαιγύ Ηε

#	Article	IF	CITATIONS
55	SIMS zircon U–Pb dating of the Late Cretaceous dinosaur egg-bearing red deposits in the Tiantai Basin, southeastern China. Journal of Asian Earth Sciences, 2013, 62, 654-661.	2.3	13
56	Magnetostratigraphy of the Dali Basin in Yunnan and implications for late Neogene rotation of the southeast margin of the Tibetan Plateau. Journal of Geophysical Research: Solid Earth, 2013, 118, 791-807.	3.4	75
57	è¾¼z西廰æ~Œç޲çぢå;"地区ä¾ç¼2—ç≌地å±,çš"ç¦»åæŽ¢é'ŕ锆石U-Pb定年: å⁻¹æœ€å ë€ å,¦ç¾¼zæ⁻>;	æé³∕ 0™ çš"ä	å¹´ä & &å^¶çº¦
58	New age determination of the Cenozoic Lunpola basin, central Tibet. Geological Magazine, 2012, 149, 141-145.	1.5	46
59	Toward age determination of the termination of the Cretaceous Normal Superchron. Geochemistry, Geophysics, Geosystems, 2012, 13, .	2.5	66
60	New 40Ar/39Ar dating results from the Shanwang Basin, eastern China: Constraints on the age of the Shanwang Formation and associated biota. Physics of the Earth and Planetary Interiors, 2011, 187, 66-75.	1.9	36
61	Palaeointensity just at the onset of the Cretaceous normal superchron. Physics of the Earth and Planetary Interiors, 2011, 187, 199-211.	1.9	18
62	Noble gas isotopes in corundum and peridotite xenoliths from the eastern North China Craton: Implication for comprehensive refertilization of lithospheric mantle. Physics of the Earth and Planetary Interiors, 2011, 189, 185-191.	1.9	63
63	Noble gas diffusion mechanism in lunar soil simulant grains: Results from 4He+ implantation and extraction experiments. Journal of Earth Science (Wuhan, China), 2011, 22, 566-577.	3.2	2
64	Chemical Zone of Nephrite in Alamas, Xinjiang, China. Resource Geology, 2010, 60, 249-259.	0.8	35
65	40Ar/39Ar dating of intrusive magmatism in the Angara-Taseevskaya syncline and its implication for duration of magmatism of the Siberian traps. Journal of Asian Earth Sciences, 2009, 35, 1-12.	2.3	34
66	SIMS U-Pb zircon age of a tuff layer in the Meishucun section, Yunnan, southwest China: Constraint on the age of the Precambrian-Cambrian boundary. Science in China Series D: Earth Sciences, 2009, 52, 1385-1392.	0.9	79
67	Toward age determination of the M0r (Barremian–Aptian boundary) of the Early Cretaceous. Physics of the Earth and Planetary Interiors, 2008, 169, 41-48.	1.9	82
68	Palaeomagnetism and 40Ar/39Ar age from a Cretaceous volcanic sequence, Inner Mongolia, China: Implications for the field variation during the Cretaceous normal superchron. Physics of the Earth and Planetary Interiors, 2008, 169, 59-75.	1.9	39
69	Petrogenesis and magma residence time of lavas from Tengchong volcanic field (China): Evidence from U series disequilibria and40Ar/39Ar dating. Geochemistry, Geophysics, Geosystems, 2006, 7, n/a-n/a.	2.5	34
70	Paleomagnetic and geochronological study of the Halaqiaola basalts, southern margin of the Altai Mountains, northern Xinjiang: Constraints on neotectonic convergent patterns north of Tibet. Journal of Geophysical Research, 2006, 111, .	3.3	10
71	Effect of gas emissions from Tianchi volcano (NE China) on environment and its potential volcanic hazards. Science in China Series D: Earth Sciences, 2006, 49, 304-310.	0.9	12
72	Intercalibration of international and domestic 40Ar/39Ar dating standards. Science in China Series D: Earth Sciences, 2006, 49, 461-470.	0.9	20

Ηυλιγύ Ηε

#	Article	IF	CITATIONS
73	Laser step-heating 40Ar/39Ar dating on young volcanic rocks. Science Bulletin, 2006, 51, 2892-2896.	1.7	8
74	40Ar/39Ar chronology and geochemistry of high-K volcanic rocks in the Mangkang basin, Tibet. Science in China Series D: Earth Sciences, 2005, 48, 1-12.	0.9	34
75	40Ar/39Ar dating of Usol'skii sill in the south-eastern Siberian Traps Large Igneous Province: evidence for long-lived magmatism. Terra Nova, 2005, 17, 203-208.	2.1	72
76	Stratigraphy and age of the Daohugou Bed in Ningcheng, Inner Mongolia. Science Bulletin, 2005, 50, 2369-2376.	1.7	53
77	Potassic Magmatism in Western Sichuan and Yunnan Provinces, SE Tibet, China: Petrological and Geochemical Constraints on Petrogenesis. Journal of Petrology, 2005, 46, 33-78.	2.8	229
78	40Ar/39Ar dating and preliminary paleointensity determination on a single lava flow from Chifeng, Inner Mongolia. Physics of the Earth and Planetary Interiors, 2005, 152, 78-89.	1.9	12
79	Paleomagnetic and geochronological constraints on the post-collisional northward convergence of the southwest Tian Shan, NW China. Tectonophysics, 2005, 409, 107-124.	2.2	50
80	Ultra-violet laser probe measurement of 40Ar/39Ar age profile in phlogopite. Science Bulletin, 2004, 49, 1949.	1.7	1
81	ISEA reversed event in the Cretaceous Normal Superchron (CNS):40Ar/39Ar dating and paleomagnetic results. Science Bulletin, 2004, 49, 926-930.	1.7	2
82	Ultra-violet laser probe measurement of40Ar/39Ar age profile in phlogopite. Science Bulletin, 2004, 49, 1949-1952.	1.7	0
83	The mass estimation of volatile emission during 1199–1200 AD eruption of Baitoushan volcano and its significance. Science in China Series D: Earth Sciences, 2002, 45, 530.	0.9	30
84	Clockwise rotations recorded in redbeds from the Jinggu Basin of northwestern Indochina. Bulletin of the Geological Society of America, 0, , B31637.1.	3.3	11
85	Light noble gas records and cosmic ray exposure histories of recent ordinary chondrite falls. Meteoritics and Planetary Science, 0, , .	1.6	5